

Extended coherently delocalized states in a frozen Rydberg gas

G. Abumwis,¹ Matthew T. Eiles,¹ and Alexander Eisfeld^{1,*}

¹*Max-Planck-Institut für Physik komplexer Systeme, Nöthnitzer Str. 38, D-01187 Dresden, Germany*

The long-range dipole-dipole interaction can create delocalized states due to the exchange of excitation between Rydberg atoms. We show that even in a random gas many of the single-exciton eigenstates are surprisingly delocalized, composed of roughly one quarter of the participating atoms. We identify two different types of eigenstates: one which stems from strongly-interacting clusters, resulting in localized states, and one which extends over large delocalized networks of atoms. These two types of states can be excited and distinguished by appropriately tuned microwave pulses, and their relative contributions can be modified by the Rydberg blockade. The presence of so many highly delocalized eigenstates could be relevant to puzzling results in several current experiments.

Assemblies of cold Rydberg atoms are ideal instruments to investigate interactions in many-particle systems. Rydberg atoms possess many readily tunable properties and can, in many circumstances, be treated with essential state Hamiltonians, easing theoretical interpretation [1–6]. Although in recent years several groups have successfully created well-defined and reproducible structures of Rydberg atoms [7–10], the most common experimental scenario is a frozen Rydberg gas [11, 12]. In such an environment, the Rydberg atoms are distributed randomly and are immobile over typical experimental timescales due to the ultracold temperature [13].

A particularly clear example of a random Rydberg gas is given by considering only two Rydberg states per atom, i.e. $\uparrow = \nu p$ and $\downarrow = \nu s$, where ν is the principal quantum number and s, p refer to the Rydberg electron’s orbital angular momentum. We consider the single-exciton sector of the full Hamiltonian, which is spanned by states $|n\rangle = |\downarrow\downarrow \dots \uparrow \dots \downarrow\rangle$. This notation implies a labeling scheme for the atoms where the sole \uparrow excitation lies at atom n . \uparrow and \downarrow atoms exchange excitation via resonant dipole-dipole interactions, resulting in collective eigenstates of the form

$$|\psi_\ell\rangle = \sum_n c_n^{(\ell)} |n\rangle. \quad (1)$$

The coefficients $c_n^{(\ell)}$ determine the extent to which $|\psi_\ell\rangle$ is coherently delocalized. For example, the random nature of the gas implies, with high probability, the existence of pairs of atoms with exceptionally short interparticle separations. These pairs can interact strongly and decouple energetically from the rest of the system, resulting in dimer states having $c_n^{(\ell)} \neq 0$ at just two atoms. These two-particle states exhibit a range of fascinating behavior and dynamics due to their strong mutual interactions. For instance, induced motion along the Born-Oppenheimer potential curves may instigate plasma formation [14, 15], or the atoms could bind into a micron-scale molecular state in a potential minimum [9, 16, 17]. The rich physics of the eigenenergy distributions has been studied extensively [18–21], but the nature of the eigenstates has remained mostly unexplored.

In this Letter we show that, in a random gas, most of the single exciton states are coherently delocalized over a large part (roughly a quarter) of the constituent atoms. Fig. 1 illustrates this result. Panels a and b depict two paradigmatic states in, for pictorial clarity, a two-dimensional gas. The amplitude of the \uparrow state at each atom is represented by the dot’s color and size. Panel (a) shows one of the dimer states previously mentioned. There exist a few other eigenstates with similarly localized dimer character; the eigenenergies of these dimers are much larger in absolute value than the mean eigenenergy. One could surmise, that the gas fragments into a hierarchy of clusters (monomers, dimers, trimers, tetramers, etc.) with corresponding eigenstates that at

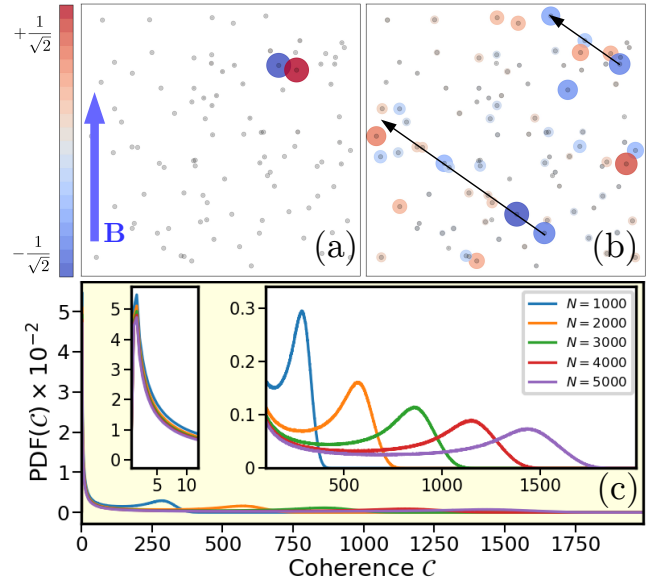


FIG. 1. (a) and (b): Two different eigenstates of the same realization. The circle size and color represents the \uparrow amplitude at each site. The magnetic field axis (blue arrow) and magic angle of the dipole-dipole interaction (black arrows) are discussed in the text. (c) The coherence probability (defined in Eq. 4) of a 3D random Rydberg gas of various sizes. The two insets highlight the low coherence (left) and high coherence (right) regions.

best are delocalize over the size of the cluster, which remains small relative to the total gas size. In contrast, the state in (b), whose eigenenergy is near the mean eigenenergy, exhibits remarkably large delocalization over many atoms.

Panel (c) shows that this delocalization is not unique to this state. Delocalization is quantified by the coherence (defined below in Eq. (4)), which indicates the number of atoms involved in a single eigenstate. Clearly, states involving around one third of the atoms are very common. In the following, we will define the relevant equations and describe our numerical simulation of the random Rydberg gas. We can then address additional aspects of the system, such as the role of the anisotropy of the dipole-dipole interaction and the possibilities to control the number of dimer states via the Rydberg blockade. These tools lead to a better understanding of this system, allowing us to revisit the delocalized states in this result in a new light.

The Hamiltonian of a random Rydberg gas takes on an appealing form when recast into the basis of single-exciton states $|n\rangle$ defined above:

$$H = \sum_{n=1}^N \epsilon_n |n\rangle\langle n| + \sum_n \sum_{m \neq n} V_{nm}(\vec{R}_n, \vec{R}_m) |n\rangle\langle m|. \quad (2)$$

In general the states $|n\rangle$ and $|m\rangle$ possess degenerate magnetic quantum number sublevels and the interaction V_{nm} has a tensorial form [18, 22, 23]. To avoid this complication we assume an applied magnetic field of around ten Gauss to isolate the $m_l = 0$ subspace via the Zeeman shift of 1.4 MHz/G [24]. The interaction then depends on R_{nm} , the interparticle distance between atoms n and m , and θ , the relative angle between \vec{R}_{nm} and \vec{B} :

$$V_{nm}(\vec{R}_n, \vec{R}_m) = \frac{\mu^2}{R_{nm}^3} (1 - 3 \cos^2 \theta). \quad (3)$$

The transition dipole between \uparrow and \downarrow states is labeled μ . Retardation effects can be neglected for the experimental parameters considered here.

Delocalization can be a challenging concept to quantify since it is not an observable, being instead a property of the wave function itself. Several complementary measures can be used to extract the most relevant information [25, 26]; two standard ones are the ‘‘inverse participation ratio’’ (IPR) [25] and the coherence [27],

$$\mathcal{C}_\ell = \sum_n \sum_{m \neq n} |\rho_{nm}^{(\ell)}| \quad (4)$$

where $\rho_{nm}^{(\ell)} = |\psi_n^{(\ell)}\rangle\langle\psi_m^{(\ell)}|$. We focus on coherence since it has a more intuitive interpretation. As a rule of thumb, its value corresponds to the number of atoms coherently sharing the \uparrow excitation. $\mathcal{C} = 1$ corresponds exactly to a dimer state.

To create eigenstates $|\psi_\ell\rangle$, one can first excite an initial ultracold gas of density n_{atom} to the state $G = |\downarrow\downarrow \dots \downarrow\rangle$.

In a typical scenario, roughly 1% of the initial unexcited atoms are promoted to the Rydberg state, and so the Rydberg density n can easily range from $10^8 - 10^{11} \text{cm}^{-3}$ [6]. For typical ultracold gas dimensions of $V \sim (100 \mu\text{m})^3$, this process results in $N \approx 1000$ Rydberg atoms. We measure distances and energies in units of mean interparticle distance $n^{1/3}$ and mean interaction strength, respectively. Although the energy scales vary with density, the eigenstates are density-independent.

To obtain a specific gas realization we simulate an atomic cloud by placing N atoms within a cube of volume L^3 following a uniform distribution. The importance of edge effects caused by the boundaries of the simulation volume is reduced for larger values of N , although we do not consider edge effects to be particularly problematic since they, to some extent, reflect the real physical boundaries of the sub-millimeter scale of the atomic cloud. Although realistic atomic clouds do not have truly uniformly distributed particles, we expect the results to be qualitatively similar. With the atomic positions simulated thusly, the Hamiltonian (Eq. (2)) is specified for that realization and can be numerically diagonalized.

At least 10^4 realizations of a random gas of N atoms are averaged to obtain the distribution of states shown in Fig. 1c. As seen in the left inset there are no states with coherence \mathcal{C} smaller than one, implying that it is impossible to excite individual atoms in the gas. Following the sudden onset at $\mathcal{C} = 1$ the coherence probability rapidly decreases at a rate nearly independent of N , before leveling off and continuing at a finite value into a very long tail (right inset). The tail extends to coherence values around one-third of N , and even increases to form a broad peak at large \mathcal{C} .

To gain more insight into this coherence distribution we investigate the correlation between eigenenergy and delocalization. Fig. 2 displays the probability to find a state with a given eigenenergy and coherence. This distribution clearly reveals that the low coherence peak in Fig. 1 is associated with large energy shifts; the energy tails (not shown at this scale) are almost exclusively dimer states with $\mathcal{C} = 1$. Since the probability to find small clusters of atoms is independent of N , so is the coherence probability over this range, as confirmed by Fig. 1c. In contrast, states with high coherence are strongly associated with states having approximately the mean interaction energy. This suggests that these large decoherences are provided by networks of mutually interacting atoms. There is also a clear asymmetry in this distribution with respect to the mean eigenenergy which is not visible in the marginal distribution.

To study this further, we take advantage of an inherent mechanism to suppress the population of dimers in a random Rydberg gas: the Rydberg blockade [28–31]. Until now we have ignored the induced dipole-dipole interaction between states of the same parity since it is far weaker ($\sim R^{-6}$) than the resonant dipole-dipole interac-

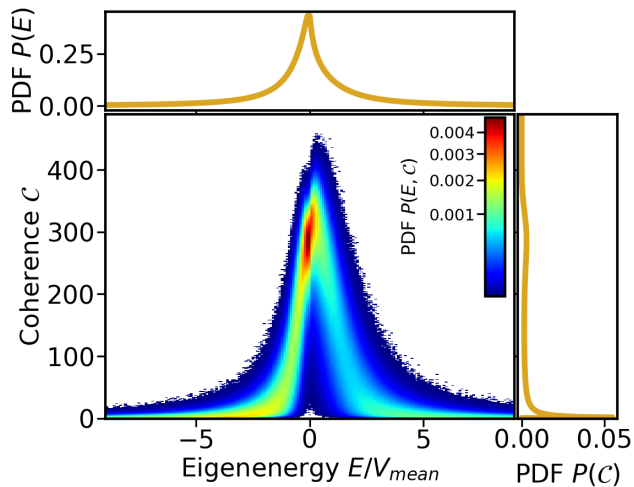


FIG. 2. Distribution of states having coherence C and eigenvalue E for $N = 1000$. The marginal distributions are plotted on the top and side.

tion ($\sim R^{-3}$). However, this interaction has a profound impact on the distribution of atomic positions making up the initial state G because the energy of the two-atom state $|\downarrow\downarrow\rangle$ is no longer equal to twice the energy of an isolated $|\downarrow\rangle$ state. Two atoms closer than the “blockade radius” can therefore not be simultaneously excited [32]. To crudely incorporate this effect we eliminate, from the initial distribution of Rydberg atom positions, one atom from each pair having a mutual separation less than one R_B . In the laboratory, varying ν or the laser bandwidth Ω can tune the blockade radius over a wide range of values, $R_B \propto (\nu^{11}/\Omega)^{1/6}$. The Rydberg blockade is a useful theoretical tool to relate localization and coherence to the interparticle separations in the gas [19]. Imposing the blockade prevents the formation of small clusters of atoms, such as the localized dimer states shown in the green circles selected in Fig. 1a. Figure 3 reveals a sharp loss in this peak at low coherence mirroring the increased suppression of clusters. As the blockade radius increases to one interparticle distance the low coherence peak is totally erased, compensated by an increase in the number of highly delocalized states.

Finally, we can examine the nature of these eigenstates by varying the strength (determined by the power-law exponent R^{-a}) and isotropy of the interaction. We merely summarize the conclusions here of a full study to be presented elsewhere [33]. For all power law potentials with $2 \leq a \leq 6$ and for both anisotropic and isotropic interactions a large population of very delocalized states with high coherence remains, but the overall delocalization strength does decrease as the interaction becomes more short-ranged. This is clearest in the peak at very large coherence, which is highly pronounced if a is less than or equal to the gas’s dimension, and gradually shrinks as a

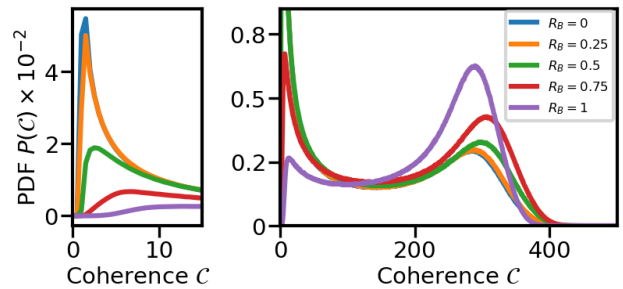


FIG. 3. Coherence probability for several Rydberg blockade radii R_B . The two panels highlight different regions and use different y -scales; the shaded region is the same in both.

increases until it vanishes completely. The distribution of eigenenergies becomes more sharply peaked near zero as a increases. We find also that increased anisotropy in the interaction increases the amount of delocalization, but this effect seems to be rather subtle and deserves further investigation. We observe that the anisotropy complicates a simple one-to-one correspondence between small interparticle distances and large interactions, and this could be a reason why extended networks featuring large decoherence are more probable for anisotropic interactions. One can guarantee that close pairs that happen to lie near the magic angle $\theta \approx 54^\circ$ of the dipole-dipole potential will only weakly interact and hence become part of extended states rather than dimers; this is manifested in the angular correlations along these rays visible in Fig. 1b.

After compiling these results together, an explanation for the formation of delocalized states emerges. It is clear that strongly localized states are associated with very strong interactions, and hence with small clusters at favorable orientations for the dipole-dipole anisotropy. These clusters decouple from and stop interacting with the rest of the system, leaving behind a residual distribution of atoms which is no longer truly uniformly distributed since it has very few remaining small clusters. The Rydberg blockade exaggerates this by even more strongly suppressing cluster formation in the initial distribution. The remaining atoms left to participate are still randomly arranged, but their spacing is more regular than allowed in a uniform distribution. Excitations therefore extend over very many atoms. We note that, as most previous effort has been devoted to the eigenvalue statistics, rather than eigenstate properties, of such random systems, this property has to the best of our knowledge only scarcely been noticed [34, 35].

Of course, these coherent delocalized states are only physically relevant if they are robust to noise or disorder. If perturbations on the order of the smallest interactions in the gas can destroy these states, then the delocalization is in some sense trivial and, more crucially, could never be realized experimentally. A sophisticated

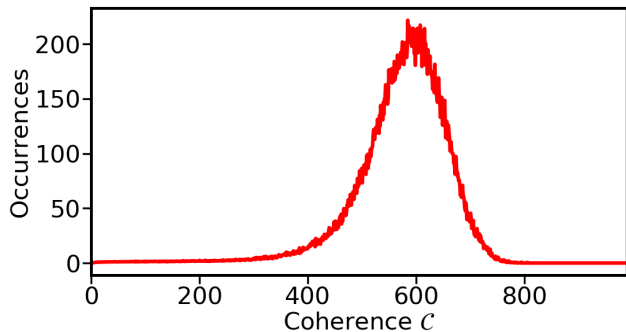


FIG. 4. Distribution of coherence values for $N = 2000$. 10^3 realizations are used, and the total number of occurrences is approximately 4×10^3 . Highly delocalized states are excited by a 500 nanosecond long microwave pulse .

study of the effects of disorder and decoherence requires a full inclusion of these effects into the evolution of the density matrix, which is beyond the scope of this Letter. Instead, as a crude check of the effects of some of these perturbations, we include diagonal disorder by adding random energy shifts to the diagonal of the Hamiltonian, or remove small off-diagonal matrix elements under some cutoff threshold. Both effects tend to suppress the long-range coherence, but we find that this suppression is not strong in this system: the localization length is only reduced by a factor of around two-thirds even when the disorder strength is on the order of one mean interaction or when interactions up to a tenth of the mean interaction are removed. This shows that these states are robust, and furthermore indicates that the interactions between various atoms contained in the delocalized states are still fairly large, which help to preserve it under perturbation.

In conclusion, we have undertaken an extensive numerical study of the properties of collective eigenstates of an excitation in a random medium with long-range interactions. We stress that our observations are generic to a variety of physical situations with long-range interactions between randomly placed particles, although the random Rydberg gas emphasized here, having naturally long-range interactions with rich angular structure, random statistics, and the mechanism of Rydberg blockade for eliminating localized states, is an ideal physical realization. As demonstrated by Figs. 1 and 3, we find that the majority of eigenstates in a random gas are highly delocalized, with coherences extending upwards of one-third of the atoms. These states can be accessed experimentally via microwave absorption: in Fig. 4 we show the distribution of coherence values which can be excited by a 500ns pulse for Rydberg states around $\nu = 60$. The microwave intensity is tuned to ensure that only highly delocalized states can be excited, showing that they can be studied selectively in typical experimental parameter regimes.

While for the strongly interacting dimer states there is quite fast motion associated [36] for the extended states we do not expect fast motion, since on the one hand the interaction is smaller than in the dimer states, on the other hand the delocalization in addition reduces the induced forces [37]. An interesting perspective is to study the resulting adiabatic and non-adiabatic dynamics of such extended states in a gas [38].

The observation that there exist strongly delocalized states with appreciable oscillator strength (of order unity) may aid in the interpretation and understanding of the phase modulation spectroscopy of very dilute gases interacting through the resonant dipole potential, although in a totally different energetic regime as these were not Rydberg atoms. In such experiments unexpectedly large signals have been observed [39] and, in the absence of a more compelling explanation, attributed to many body effects [40, 41]. The delocalized states that we find here can greatly amplify such signals. Although a full explanation requires a study of the two or more exciton system, preliminary studies indicate that the 2-exciton states have a coherence length that scales as $N^2/4$. The Rydberg parameter range explored here allows one to perform similar experiments under a more controlled setting to try to unravel this puzzle.

We acknowledge funding from the DFG: grant EI 872/4-1 through the Priority Programme SPP 1929 (GiRyd). AE acknowledges support from the DFG via a Heisenberg fellowship (Grant No EI 872/5-1). MTE acknowledges support from the Max-Planck Gesellschaft via the MPI-PKS visitors program and from an Alexander von Humboldt Stiftung postdoctoral fellowship.

* eisfeld@pks.mpg.de

- [1] A. Browaeys, D. Barredo, and T. Lahaye, *Journal of Physics B: Atomic, Molecular and Optical Physics* **49**, 152001 (2016).
- [2] T. F. Gallagher, *Rydberg Atoms* (Cambridge University Press, Cambridge, England, 2005).
- [3] M. D. Lukin, M. Fleischhauer, R. Cote, L. M. Duan, D. Jaksch, J. I. Cirac, and P. Zoller, *Physical Review Letters* **87** (2001), 10.1103/physrevlett.87.037901.
- [4] A. Browaeys and T. Lahaye, in *Niels Bohr, 1913-2013* (Springer International Publishing, 2016) pp. 177–198.
- [5] M. Saffman, T. G. Walker, and K. Molmer, *Rev. Mod. Phys.* **82**, 2313 (2010).
- [6] T. Liebisch, M. Schlagmüller, F. Engel, H. Nguyen, J. Balewski, G. Locheid, F. Böttcher, K. M. Westphal, K. S. Kleinbach, T. Schmid, A. Gaj, R. Löw, S. Hofferberth, T. Pfau, J. Pérez-Ríos, and C. H. Greene, *Journal of Physics B: Atomic, Molecular and Optical Physics* **49**, 182001 (2016).
- [7] D. Ohl de Mello, D. Schäffner, J. Werkmann, T. Preuschoff, L. Kohfahl, M. Schlosser, and G. Birkel, *Phys. Rev. Lett.* **122**, 203601 (2019).
- [8] H. Bernien, S. Schwartz, A. Keesling, H. Levine, A. Om-

- ran, H. Pichler, S. Choi, A. S. Zibrov, M. Endres, M. Greiner, V. Vuletić, and M. D. Lukin, *Nature* **551**, 579 (2017).
- [9] S. Hollerith, J. Zeiher, J. Rui, A. Rubio-Abadal, V. Walther, T. Pohl, D. M. Stamper-Kurn, I. Bloch, and C. Gross, *Science* **364**, 664 (2019), <https://science.sciencemag.org/content/364/6441/664.full.pdf>
- [10] D. Barredo, V. Lienhard, S. de Léséleuc, T. Lahaye, and A. Browaeys, *Nature* **561**, 79 (2018).
- [11] I. Mourachko, D. Comparat, F. de Tomasi, A. Fioretti, P. Nosbaum, V. M. Akulin, and P. Pillet, *Phys. Rev. Lett.* **80**, 253 (1998).
- [12] W. R. Anderson, J. R. Veale, and T. F. Gallagher, *Phys. Rev. Lett.* **80**, 249 (1998).
- [13] F. Robicheaux, J. V. Hernández, T. Topçu, and L. D. Noordam, *Physical Review A* **70** (2004), 10.1103/physreva.70.042703.
- [14] W. Li, M. W. Noel, M. P. Robinson, P. J. Tanner, T. F. Gallagher, D. Comparat, B. Laburthe Tolra, N. Vanhaecke, T. Vogt, N. Zahzam, P. Pillet, and D. A. Tate, *Phys. Rev. A* **70**, 042713 (2004).
- [15] W. Li, P. J. Tanner, and T. F. Gallagher, *Phys. Rev. Lett.* **94**, 173001 (2005).
- [16] H. Saßmannshausen and J. Deiglmayr, *Phys. Rev. Lett.* **117**, 083401 (2016).
- [17] C. Boisseau, I. Simbotin, and R. Côté, *Phys. Rev. Lett.* **88**, 133004 (2002).
- [18] F. Robicheaux, J. V. Hernández, T. Topçu, and L. D. Noordam, *Physical Review A* **70**, 042703 (2004).
- [19] T. Scholak, T. Wellens, and A. Buchleitner, *Phys. Rev. A* **90**, 063415 (2014).
- [20] A. Goetschy and S. E. Skipetrov, *Phys. Rev. E* **84**, 011150 (2011).
- [21] A. Goetschy and S. E. Skipetrov, *arXiv:1303.2880* (2013).
- [22] H. Park, P. J. Tanner, B. J. Claessens, E. S. Shuman, and T. F. Gallagher, *Phys. Rev. A* **84**, 022704 (2011).
- [23] S. Möbius, S. Wüster, C. Ates, A. Eisfeld, and J.-M. Rost, *J. Phys. B* **44**, 184011 (2011).
- [24] D. Barredo, H. Labuhn, S. Ravets, T. Lahaye, A. Browaeys, and C. S. Adams, *Phys. Rev. Lett.* **114**, 113002 (2015).
- [25] B. Kramer and A. MacKinnon, *Rep Prog Phys* **56**, 1469 (1993).
- [26] L. Gong, W. Li, S. Zhao, and W. Cheng, *Physics Letters A* **380**, 59 (2016).
- [27] T. Baumgratz, M. Cramer, and M. B. Plenio, *Phys. Rev. Lett.* **113**, 140401 (2014).
- [28] D. Jaksch, J. I. Cirac, P. Zoller, S. L. Rolston, R. Côté, and M. D. Lukin, *Physical Review Letters* **85**, 2208 (2000).
- [29] D. Tong, S. Farooqi, J. Stanojevic, S. Krishnan, Y. Zhang, R. Côté, E. Eyler, and P. Gould, *Physical Review Letters* **93**, 063001 (2004).
- [30] A. Gaëtan, Y. Miroshnychenko, T. Wilk, A. Chotia, M. Viteau, D. Comparat, P. Pillet, A. Browaeys, and P. Grangier, *Nature Physics* **5**, 115 (2009).
- [31] E. Urban, T. A. Johnson, T. Henage, L. Isenhower, D. Yavuz, T. Walker, and M. Saffman, *Nature Physics* **5**, 110 (2009).
- [32] We ignore the anisotropy that can, depending on the atomic states being considered, be present in the induced van der Waals interaction.
- [33] Abumwis *et al* in preparation.
- [34] T. Scholak, T. Wellens, and A. Buchleitner, *Physical Review A* **90**, 063415 (2014).
- [35] S. E. Skipetrov and A. Goetschy, *Journal of Physics A: Mathematical and Theoretical* **44**, 065102 (2011).
- [36] W. Li, J. P. Tanner, Y. Jamil, and F. T. Gallagher, *Eur. Phys. J. D* **40**, 27 (2006).
- [37] C. Ates, A. Eisfeld, and J.-M. Rost, *New J. Phys.* **10**, 045030 (2008).
- [38] S. Wüster, A. Eisfeld, and J.-M. Rost, *Phys. Rev. Lett.* **106**, 153002 (2011).
- [39] L. Bruder, M. Binz, and F. Stienkemeier, *Phys. Rev. A* **92**, 053412 (2015).
- [40] Z.-Z. Li, L. Bruder, F. Stienkemeier, and A. Eisfeld, *Phys. Rev. A* **95**, 052509 (2017).
- [41] L. Bruder, A. Eisfeld, U. Bangert, M. Binz, M. Jakob, D. Uhl, M. Schulz-Weiling, E. R. Grant, and F. Stienkemeier, *Phys. Chem. Chem. Phys.*, 2276 (2019).